Asymptotical Performance of Ring Based Routing for Wireless Sensor Networks with a Mobile Sink: An Analysis

Sheng Yu[1], Baoxian Zhang[1(✉)], Chunxi Li[2], Kun Hao[3], and Cheng Li[3,4]

[1] University of Chinese Academy of Sciences, Beijing 100049, China
yusheng08@mails.ucas.ac.cn, bxzhang@ucas.ac.cn
[2] Beijing Jiaotong University, Beijing 100044, China
chxlil@bjtu.edu.cn
[3] School of Computer and Information Engineering, Tianjin Chengjian University, Tianjin, China
littlehao@126.com
[4] Memorial University of Newfoundland, St. John's, NL A1B 3X5, Canada
licheng@mun.ca

Abstract. Design of efficient routing protocols has been a critical issue in wireless sensor networks with mobile sinks (mWSN). In [1], Yu et al. proposed a distributed lightweight ring based routing protocol for mWSNs, which builds a multi-ring based network structure by creating a quasi-polar coordinate system on the network in order to support efficient ring based routing. However, in [1], only average case routing performance was reported via simulations. In this paper, we derive the asymptotical path-length performance of the ring based routing via extensive analyses. We hope the results reported in this paper can be helpful for understanding the characteristics of ring based routing.

Keywords: Wireless sensor network · Mobile sinks · Distributed routing

1 Introduction

Wireless sensor networks with mobile sinks (mWSN) have the potential to be used in many applications such as military operations, commercial, patrols, environment monitoring, and etc. Design and evaluation of mWSNs have received a lot of attention recently and much work has been carried out [1]. An mWSN typically consists of many static sensor nodes and one or more mobile sink nodes (MSs). Efficient routing for achieving high routing performance in mWSNs has been a critical issue.

This work was supported by National Natural Science Foundation of China under Grant Nos. 61471339 and 61531006, 61572071, U1534201, and the Natural Sciences and Engineering Research Council (NSERC) of Canada (Discovery Grant 293264-12), and InnovateNL SensorTECH project 5404-2061-101.

J. Zheng et al. (Eds.): ADHOCNETS 2018, LNICST 258, pp. 93–104, 2019.
https://doi.org/10.1007/978-3-030-05888-3_9

Existing routing protocols for mWSNs can be divided into location based protocols and topology based routing. In location based routing, location information of mobile sink is used to assist geographical packet forwarding. In [2], an Adaptive Location Update based Routing Protocol (ALURP) was presented to restrict the scope of location updates caused by sink mobility to a small area (called destination area) with slight sacrifice on routing distance performance. The Elastic Routing (ER) protocol [3] enables a source sensor node to keep obtaining the up-to-date location information of a mobile sink during its continuous data reporting to the sink. In [4, 5], the authors focused on how to design efficient location services for providing fresh location information of a nearby mobile sink to a sensor node with data to report while having low protocol overhead, where [4] presented a flat location service while [5] presented a hierarchical location service. Topology based routing protocols can be further divided into proactive routing protocols (e.g., AVRP [6] and MDRP [7, 8]) and reactive routing (e.g., TRAIL [6] and DDRP [9]). In proactive routing protocols, data paths from sensor nodes to mobile sink need to be established and updated from time to time, which can cause a lot of protocol overhead for route maintenance. In reactive routing protocols, overhearing on wireless channels (e.g., the passing of an MS in TRAIL [6] and transmission of a data packet in the neighborhood in DDRP [9]) is often used for path learning with minimal protocol overhead. When no such overhearing opportunity is available or previously learnt routes are outdated, random walk has to be triggered.

In [1], Yu et al. proposed an efficient lightweight reactive routing protocol called R3, which integrates ring-based routing and trail-based routing. R3 does not require location information to be kept at nodes in the network. In R3, a data packet is forwarded by using ring-based routing until it reaches a mobile sink or can be forwarded to a mobile sink along a fresh trail along which the sink moves. To support efficient ring-based routing/forwarding, R3 builds a multi-ring-based infrastructure on a multihop wireless sensor network when the network is initially deployed by creating a quasi-polar coordinate system on the network. When performing packet forwarding on a particular ring, the next hop leading to the maximum angle progress is chosen until reaching a mobile sink (or an agent node recruited by a mobile sink, or a fresh trail to reach a mobile sink). When the searching on a particular ring failed, another ring will be tried. This process continues until a mobile sink is found or no mobile sink can be found after pre-determined number of rings are tried. In [1], simulation results show that the R3 protocol outperforms existing work on average in different scenarios.

However, in [1], only average-case performance was reported. How long a shortest path along a ring, in the best and worst case, could be is not answered. In this paper, we shall tackle this issue via extensive analyses. We hope the results reported in this paper can be helpful for understanding the characteristics of ring based routing in an mWSN.

2 The R3 Protocol

The R3 protocol [1] is a lightweight distributed routing protocol targeted for mWSNs. The protocol only requires each node keep very limited routing information, which includes its node id, ring id, angle, gradient, and also its one-hop neighbor list. To support efficient data routing, R3 adopts ring-based forwarding. More specifically, each

data packet is forwarded using ring-based forwarding until it reaches a mobile sink. A ring is formed by a number of nodes, all of which have the same hop distance to a base ring in the network and are expected to form an annulus for assisting packet forwarding. Packet forwarding along such an annulus is referred to as ring-based forwarding.

The network model used in R3 is as follows. A wireless multihop network can be modelled by $G(V, E)$, where $V(G)$ is constituent of one or multiple mobile sink nodes and multiple static sensor nodes and $E(G)$ represents the set of links in the network. Sensor nodes and sink nodes have the same communication range R. For each pair of nodes $u, v \in V(G)$, we have link $(u, v) \in E(G)$ if $d_{uv} \leq R$; otherwise $(u, v) \notin E(G)$. we let d_{uv} represent the geometrical distance between node u and node v. Each node is equipped with a omni-directional antenna. Nodes are uniformly deployed in a two-dimensional sensing field. Each mobile sink node moves randomly and freely in the sensing field. Nodes do not have their location information.

To support ring-based forwarding, the R3 protocol needs to first build a multi-ring-based structure on a wireless multihop sensor network when the network is initially deployed. The ring-based structure creation contains three rounds of (signaling) flooding operations. The first round of flooding prepares gradient information for sensor nodes in the WSN. To achieve this goal, a designated root node (e.g., a sensor node near the center of the WSN, see the node at the center point in Fig. 1 in our example) is chosen to start the flooding of a signaling message across the network, which enables each sensor node in the network to learn its hop distance to the designated root node as its gradient value. The second round of flooding is to build a base ring and is initiated by a sensor node with gradient of two. This round of flooding identifies a shortest cycled min-hop path, which tightly embraces a *virtual* topological hole that is artificially created in the central area of the network. This cycled shortest path is treated as the *base ring*. In the implementation of R3, all the nodes with gradients 1 and 0 (as identified in the first round of flooding operation) form the virtual hole. In Fig. 1, all the nodes in the most inner circle form the virtual hole. When multiple such cycled paths are found, the path leading to the min hop distance is chosen. In Fig. 1, the yellow nodes form the base ring. Each of the remaining (outer) rings is constituted of those sensor nodes having the same hop distance to the base ring. For example, in Fig. 1, all the green nodes have hop distance of one to the base ring. Similarly, those red, blue, and deepred nodes form each of the remaining outer rings. The creation of outer rings can be accomplished by a third round of flooding, triggered by nodes on the base ring. It should be noted that to ease the understanding and also for simplicity of illustration, in Fig. 1, each ring appears as a circular annulus. However, in reality, since the distance between different rings are measured in hops instead of geometrical distance, nodes in a ring does not necessarily form a circular annulus.

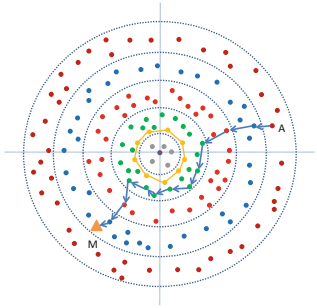

Fig. 1. Example illustrating how the R3 protocol works.

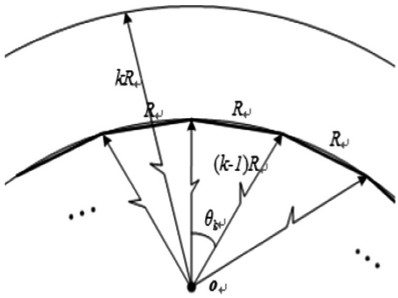

Fig. 2. Illustration of the shortest path in the best case on the *k*-th ring.

When carrying out ring-based packet forwarding, data packets are forwarded along nodes on a pre-selected ring along a pre-determined direction (either clockwise direction or anticlockwise direction). To enable data packets to be able to steadily move along the same direction and also minimize the path distance, virtual angle information is assigned to sensor nodes in the network in the following way: Nodes on the base ring are first assigned with virtual angles based on their positions on the cycled path (measured by their hop distances to a preselected reference node on the base ring, which can be randomly selected from nodes on the base ring, all in the same direction). In Fig. 1, suppose the lower most node in the base ring is chosen as the reference node with degree 0, then the other eight nodes in the base ring will respectively have degrees (in the closewise direction): 40°, 80°, 120°,…, 320°. The virtual angles of nodes on other outer rings are iteratively computed based on the virtual angles of their neighbor nodes (can also be seen as their farther nodes) on their immediate inner rings. In this way, a polar coordinate system can be built by assigning each node the following information: (1) a ring ID based on its distance to the base ring, and (2) a virtual angle. Such ring based structure is required to be created only once and at the network initialization phase and accordingly very limited extra protocol overhead is generated.

When performing actual packet forwarding along a selected ring, the next hop leading to max angle progress (on pre-selected direction, i.e., either clockwise direction or anti-clockwise direction) is always chosen. This hop by hop packet forwarding process continues until the packet reaches a mobile sink. A mobile sink can recruit agent nodes on the ring-based structure, one on each ring, to increase the successful probability to find mobile sink on a selected ring. When the MS searching process on a chosen ring fails, another ring will be tried. This process continues until a mobile sink is found or no mobile sink can be found when pre-determined number of rings are tried. Figure 1 shows how such ring-based forwarding can work for a sensor node A to send a packet to mobile sink M. For more details regarding how R3 works, please refer to [1].

Extensive simulation results in [1] show that R3 outperforms existing work in different scenarios. However, [1] only reported R3's average-case performance. How long a shortest path by such ring based forwarding, in the best and worst case, could be is not answered. In this paper, we shall address this issue via extensive analyses.

3 Analytical Results

This section analyzes how long a shortest route along a ring by R3 could be, in the best and worst case, respectively.

***Lemma* 1:** For a path $P = (s = 1, 2, 3, \ldots, K-1, K = t)$, which is a path on a particular ring returned by R3, we have: For any nodes x, $y \in P$, $y \geq x+2$, we have $d_{xy} > R$. That is, the geometrical distance between any pair of non-neighbor nodes on P must be larger than R.

This is obvious because otherwise removal of those node(s) sitting between x and y from path P would have led to a shorter path by R3. More specifically, if $d_{xy} \leq R$ holds, the decision that node x had not chosen node y as its next hop would have violated R3's forwarding policy that each node should choose its neighbor with the maximum angle progress as its next hop. The holding of *Lemma* 1 also means that, for each node $x \in P$, we have that node $x + 2$ and its descendant nodes on P must have left x by at least R^+ distance on the anticlockwise side, where R^+ equals R plus positive infinitesimal.

Next, we present some results on the length of a shortest path constituent of nodes on a particular ring. It is easy to derive that, on a very sparse and irregular network, the length of such a path can be arbitrarily long, i.e., in the worst case, $O(|V|)$. In our analysis below, we assume that the network is densely distributed such that there exists a node at arbitrary position. For such a dense network, the width of each ring is obviously exactly R. Let o represent the common center of all the rings. To ease the analysis below, with a slight abuse of notation, for the k-th ($k \geq 2$) ring, we say it cover the space between two neighboring concentric circles, both of which are centered at o but have radius $(k-1)R$ and kR, respectively. We call the circle with radius $(k-1)R$ as its inner circle and the circle with radius kR its outer circle. Obviously, the so-called *base* ring identified by R3 is located in the 2nd ring. In our analysis below, we assume the exact location of each point in the network is known.

Next, we analyze the length of a shortest path to finish the travel (a closed tour) along a k-th ring ($k \geq 2$), in the best and worst case, respectively. The key factor affecting the length of such a path is the average central angle that each hop on such a path can cover. To obtain the best-case shortest path, we wish each hop to obtain the maximum angle progress. In contrast, to obtain the worst-case shortest path, we wish each hop (on average) to obtain the minimum angle progress. Note that the R3 protocol pursues short paths whenever available, by using one-hop topological information kept at each node.

Result 1: A fastest way to finish a closed tour along the k-th ring ($k \geq 2$) is that each hop advances R distance along a circle centered at o with the minimum radius on the ring, unless the last hop, which may not be that long. Let N_{min}^k denote the length of the shortest path in the best case in the k-th ring, we have

$$N_{min}^k = \left\lfloor \frac{2\pi}{cos^{-1}\left(\frac{2(k-1)^2-1}{(k-1)^2}\right)} \right\rfloor + 1, \forall k \geq 2. \quad (1)$$

Figure 2 illustrates how N_{min}^k can be obtained. For the k-th ring, its inner circle is a circle centered at o with a radius $(k-1)R$. The maximum angle progress each hop can make is when two nodes are located on the inner circle and the distance between them are exactly R. Let θ_k denote that maximum angle progress that a single hop can obtain in the k-th ring. Based on the cosine theorem, we have the following equation

$$\theta_k = \cos^{-1}\left(\frac{2(k-1)^2-1}{2(k-1)^2}\right), \forall k \geq 2. \tag{2}$$

It directly follows from the above equation that in the best case, the length of the shortest path is $\left\lfloor \frac{2\pi}{\theta_k} \right\rfloor + 1$ hops in the k-th ring. Table 1 shows some values of N_{min}^k.

Table 1. Values of N_{min}^k.

k	2	3	4	5	6	7
N_{min}^k	7	13	19	26	32	38

The deduction of the worst-case length of a shortest path along a ring, however, is not easy. The key point is how slow we can achieve for traveling along such a ring along a fixed direction. *Lemma* 1 puts certain restriction on the slowness of the travel. Based on how the fastest path is created, an intuition is that at each hop, the path head node only moves forward $R/2$ (plus infinitesimal) distance instead of R (as done for creating the fastest path). This strategy works if we wish to travel along a curve or a line. We name this strategy as curve-based strategy. However, the worst case for traveling along a circular slice with certain width can be much worse than that due to the curve-based strategy because we can take a zigzag path along such a slice. To illustrate this, we provide such an example in Fig. 3(a).

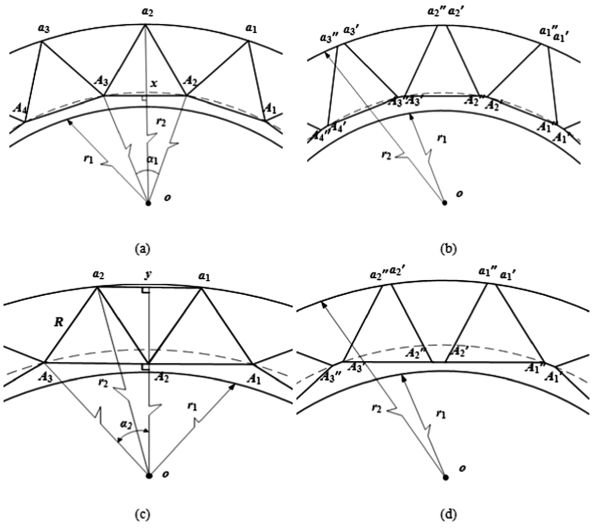

Fig. 3. Cases that equilateral triangles are tightly arranged in an annulus.

In Fig. 3(a), all the equilateral triangles are arranged on the dashed circle which makes one vertex of each of the equilateral triangles is on the outer circle of the ring and their height is exactly $\sqrt{3}R/2$. The side length of all the equilateral triangles is R. In Fig. 3(b), we further expand every vertex of the equilateral triangles to two nodes with a distance δ between them, where δ is positive infinitesimal. Note that in this expanding process, the length of each segment (A_i'', A_{i+1}'), $\forall i$, is also expanded from R to $R + \delta$, all in the same direction. This extra expansion is to keep *Lemma* 1 not violated in later path discovery. We are interested in the length of path $A_1'A_1''a_1'a_1''A_2'A_2''a_2'a_2''\ldots\ldots$ as $\delta \rightarrow 0+$ or equivalently, how many such equilateral triangles can be tightly arranged along the dashed circle. Obviously, traveling in such a zigzag manner and with such node expansions can lead to a path with a length approximately double to that due to the previously mentioned curve-based strategy[1]. We name this way of travel arrangement as triangle-based strategy. Next, we derive how many equilateral triangles can be tightly arranged on the dashed circle. Suppose the ring under study is the k-th ring, then the radius of its inner circle $r_1 = (k-1)R$. Let x denote the middle point of line segment $\overline{A_2A_3}$ (see Fig. 3(a)). Consider the triangle A_2oA_3, we need to calculate its associated central angle $\angle A_2oA_3$. Note that $\overline{xo} = \overline{oa_2} - \overline{xa_2} = kR - \sqrt{3}R/2$. Let α_1 represent $\angle A_2oA_3$. We have $\overline{xA_3} = \overline{xA_2} = R/2$. Note $\angle oxA_3$ is a right angle and $\alpha_1 = 2\angle xoA_3$, thus

$$\alpha_1 = 2\tan^{-1}\left(\frac{\overline{xA_3}}{\overline{xo}}\right) = 2\tan^{-1}\left(\frac{1}{2k-\sqrt{3}}\right) \tag{3}$$

The number of equilateral triangles that can be arranged on the dashed circle in Fig. 3(a), denoted by M_1, is bounded by the following inequality,

$$\left\lfloor \frac{2\pi}{\alpha_1} \right\rfloor \leq M_1 \leq \left\lceil \frac{2\pi}{\alpha_1} \right\rceil. \tag{4}$$

Since we are interested in the worst case, we choose

$$M_1 = \left\lceil \frac{2\pi}{\alpha_1} \right\rceil \tag{5}$$

Thus, the maximum hops of a shortest path (closed tour) on such a ring due to the scenario shown in Fig. 3(a) (denoted by N_1) is as follows.

$$N_1 = 4 \times M_1 \tag{6}$$

[1] In the analysis, we ignore the impact of the last triangle problem, which may not be well nested there and thus lead to a few less hops on the worst-case shortest path derived based on number of equilateral triangles. Since we here focus on how worse, in the extreme case, the length of a shortest path taken by ring-based routing could be, the impact of the last triangle is ignored. Similar strategy will also be used in later analysis.

In the above expansion process, each node can only be expanded to two nodes, which are infinitely close to each other. Expanding a node to three or more such nodes will make a path containing such expanded nodes directly violate *Lemma* 1 and is thus unacceptable. Also, in Fig. 3, it is seen that the distance between original nodes (i.e., those nodes before expansions) should be exactly R (for neighbors) or larger (for non-neighbors). Let's again take a look at a triangle $\Delta A_1 a_1 A_2$ in Fig. 3(a), increasing $\overline{A_1A_2}$ further will make the triangle unnecessarily cover larger angle or central angle (i.e., $\angle A_1 o A_2$), which would cause length reduction in the worst-case path; in contrast, decreasing $\overline{A_1A_2}$ to be smaller than R will cause violation of *Lemma* 1 because the distance between the expanded nodes of A_1 and those of A_2 will be shorter than R. This is why equilateral triangle can well characterize the relationship among each group of three original nodes $A_i a_i A_{i+1}$. In Figs. 3(a) and (b), we have seen the power of expanding nodes in such a way for creating long paths. The purpose of such expansion is to maximally slow down the travel along a long slice at each step before proceeding further and it can easily double the worst-case path length at almost no cost.

Let us proceed to consider another extreme case as shown in Fig. 3(c) which may lead to a longer worst-case path than that shown in Fig. 3(a). We first place an equilateral triangle $a_2A_2a_1$ with its two vertices a_1a_2 located on the outer circle, then we arrange two additional equilateral triangles, one on each side of $\Delta a_2A_2a_1$ with a_2A_2 and A_2a_1 as one edge of them, respectively. We then repeat this pattern as shown in Fig. 3 (c). Intuitively, it looks like dragging the nodes a_1 and a_2 in Fig. 3(a) closer along the outer circle until their distance is reduced to R. Also, it can be easily derived that $A_1a_1a_2A_2$ is an equiangular trapezoid. In Fig. 3(d), we expand each vertex in Fig. 3(c) into two nodes with a distance δ in between like we did in Fig. 3(b). We are again interested in the length of the zigzag path $A_1'A_1''a_1'a_1''A_2'A_2''a_2'a_2''\ldots$, and how many equilateral triangles can be tightly arranged in the k-th ring as $\delta \to 0^+$ without violating *Lemma* 1. This is decided by the central angle associated with a triangle, which is the angle $\alpha_2 = \angle A_2 o A_3$ (see Fig. 3(c)). Let y denote the middle point of line segment $\overline{a_1a_2}$. Note that $\angle oA_2A_3$ and $\angle oya_2$ are both right angles, $\overline{oa_2} = kR$, and $\overline{A_2A_3} = R$. Based on the Pythagorean Theorem, we have

$$\alpha_2 = \tan^{-1}\frac{\overline{A_2A_3}}{\overline{A_2o}} = \tan^{-1}\frac{R}{\sqrt{k^2R^2 - \frac{R^2}{4} - \frac{\sqrt{3}}{2}R}} = \tan^{-1}\frac{2}{\sqrt{4k^2 - 1} - \sqrt{3}}. \tag{7}$$

The number of subgraphs that can be arranged in the annulus in Fig. 3(c) in the worst case, denoted by M_2, is as follows.

$$M_2 = \left\lceil \frac{2\pi}{\alpha_2} \right\rceil \tag{8}$$

So the maximum number of hops of a shortest path (closed tour) on a ring due to the scenario shown in Fig. 3(c) (denoted by N_2) is as follows.

$$N_2 = 4 \times M_2 \tag{9}$$

By comparing (3) and (7), we have the following lemma:

Lemma 2. $\alpha_2 < \alpha_1$, for $\forall k \geq 2$.

Lemma 2 can be easily derived from (3) and (7) by using trigonometry. Following the *Lemma* 2, (6), and (9), we have

$$N_1 \leq N_2 (\forall k \geq 2). \tag{10}$$

It is interesting to ask whether N_2 is the length of the shortest path in the worst case. Figure 4 shows another extreme case such that one side of each of the equilateral triangles is parallel to a radius of the ring. Intuitively, it looks like pushing nodes a_1 and a_2 in Fig. 3(a) together until they merge to one node. Figure 4(a) shows how we arrange the equilateral triangles. In Fig. 4(a), A_i, B_i, o, $\forall i$, are on the same line. We group two neighboring equilateral triangles together and called them a subgraph. We are again interested in how many such subgraphs can be embedded into a circular slice without violating *Lemma* 1. In Fig. 4(b), like what we have done in Fig. 3(b), we expand each vertex of the equilateral triangles into two nodes with a distance δ between them[2].

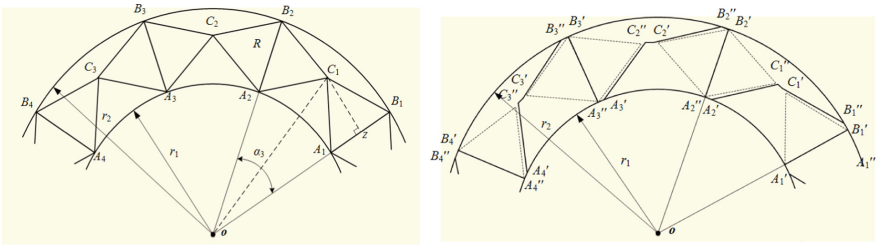

(a) (b)

Fig. 4. Cases that equilateral triangles are perpendicular to radius of the ring.

We are interested in the length of path $A_1' A_1'' B_1' B_1'' C_1' C_1'' A_2' A_2'' B_2' B_2'' \ldots\ldots$ when $\delta \rightarrow 0+$. Note that in Fig. 4(a), lowering down C_i (even slightly) would cause a violation of *Lemma* 1 since the distance between A_i and C_i would be smaller than R; In contrast, moving up a node C_i would unnecessarily increase the central angle $\angle A_{i+1} o A_i$. This is the reason why we choose to use equilateral triangles here. Next, we shall deduce the value of α_3. Note that $\overline{zo} = (k - 0.5)R$, $\overline{C_1 z} = \sqrt{3}R/2$, and $\angle C_1 zo = \pi/2$. Thus, $\angle C_1 oz = \tan^{-1}(\frac{\overline{C_1 z}}{(k-0.5)R}) = \tan^{-1}(\frac{\sqrt{3}}{2k-1})$. We have

[2] Actually, in the expansion, B_i' ($\forall i$) should also be put (moved) to the anticlockwise side of line oA_i'' with a distance ε = infinitesimal in order to keep $\overline{A_i'' B_i'} \equiv R$ because all the points on inner circle actually do not belong to the current ring under study. Because this extra procedure has no (or negligible) impact on the *asymptotical* performance, we will not discuss its impact later and simply assume o, A_i'', B_i' are on the same line and $\overline{A_i'' B_i'} \equiv R$, $\forall i$.

$$\alpha_3 = \angle C_1 o A_1 + \angle C_1 o A_2 = 2 \times \angle C_1 o z = 2 \times \tan^{-1}(\frac{\sqrt{3}}{2k-1}). \quad (11)$$

The number of subgraphs that can be arranged along a circular slice in the worst case in Fig. 4(a), denoted by M_3, is as follows.

$$M_3 = \left\lceil \frac{2\pi}{\alpha_3} \right\rceil \quad (12)$$

Thus, the maximum number of hops of a shortest path (closed tour) on a ring due to the scenario shown in Fig. 4(a) (denoted by N_3) is as follows.

$$N_3 = 6 \times M_3 \quad (13)$$

Based on (9), (10), and (13), we have a lower bound on the worst-case length of a shortest path along the k-th ring, denoted by N^k_{max}, as follows.

$$N^k_{max} = max\{N_2, N_3\}. \quad (14)$$

In reality, we may imagine to take a ring tour using quadrilateral style (e.g., squares with side R). Figure 5(a) shows such a case. However, the scenario in Fig. 5(a) will not lead to a longer worst-case path than that due to the previously used strategies because the distance between C_1 and B_2 is smaller than R such that for each square we can only visit three of its four vertices, which makes the resulting path shorter than that due to Fig. 3(a) because the dashed circle in Fig. 3(a) is longer than the inner circle used in Fig. 5(a) for arranging the squares. Or otherwise, we need to separate the squares in a way such that the distance between the closest vertices belonging to neighboring squares is exactly R (see Fig. 5(b)). In this case, a path (tour) can cover all the vertices of each square. However, it can be easily deduced that such a path is still shorter than that shown in Fig. 3(a). Note that the scenario shown in Fig. 4(a) can also be explained as a traversal of a series of identical quadrilaterals if we treat $C_iB_{i+1}C_{i+1}A_{i+1}$ (e.g., $C_1B_2C_2A_2$) as a quadrilateral and in this case, we traverse two sides and a diagonal of it. Furthermore, other regular polygons (e.g., pentagon, hexagon, etc.) are not possible to be embedded into a ring without violating *Lemma* 1 due to the limited ring width if their side length is set to R.

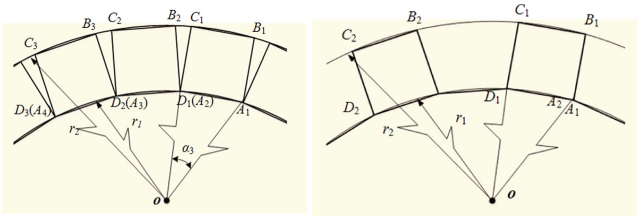

Fig. 5. Cases that quadrilaterals are arranged along the inner circle.

Now, we wish to know how close N_{max}^k obtained by using (14) is to the worst-case path length. Regarding this, we have the following. In Figs. 3 and 4, it is seen that the returned path, if excluding the impact of the last triangle (or called subgraph) problem, consists of two types of links, type I has length δ and type II has length R and these two types of links appear alternately on the path. The length of each link belonging to type II needs to be exactly R, or otherwise violation of *Lemma* 1 will be seen when node expansion is done. Accordingly, we have the following. For the two endpoints of an individual link to be expandable, the length of the link must be exactly R, otherwise, violation of *Lemma* 1 will be seen. Then, we have the following.

Observation 1: One way for creating the worst-case path is to identify a longest path consisting of original nodes (i.e., nodes before expansion) while meeting *Lemma* 1 and further keeping the distance between each pair of neighbor nodes on the path is exactly R, and then expand each original node to two nodes as we described earlier. The resulting path will be the worst-case path falling into our interest.

Observation 2: The worst-case shortest path can be obtained due to a number of identical subgraphs due to the isotropic property of a ring, if we ignore the last subgraph problem. Moreover, each subgraph itself should be symmetric with respect to a radius of the ring, in which case no extra distance (penalty) for conjunction of neighboring subgraphs will be introduced; otherwise, extra distance must be taken like the case in Fig. 5(b). For each of the identical subgraphs, we wish to traverse all its vertices (in the anticlockwise direction) along its sides and/or diagonals. Each of the traversed sides/diagonals should have length R for their endpoints to be expandable.

Obviously, all the scenarios shown in Figs. 3, 4, and 5 meet the above observations. Furthermore, using other types of quadrilateral (e.g., parallelogram, trapezoid, except those used in Figs. 3(c) and 4(a)) for guiding the tour would not lead to longer path than that using square (see Fig. 5) or parallelogram (see Fig. 4) since they will either unnecessarily occupy larger angles or not symmetric such that conjunction of neighboring such units will cause unnecessary extra costs. In this sense, we have reached a close lower bound for the longest closed tour using triangles and quadrilateral, while other polygons like pentagon, hexagon, etc., will not lead to worse paths as we discussed earlier. In this sense, we say the N_{max}^k obtained by (14) is a close lower bound on the worst-case path length for a closed shortest tour along a ring.

Result 2: Based on (14), it can be easily known that the base ring, in the best case, contains 7 hops and, in the worst case, it can contain at least 36 hops.

The base ring is a shortest cycled path on the 2nd ring. Based on the results in Table 1, we can know that the base ring, in the best case, can contain 7 hops. Based on (9), $N_2 = 36$, and based on (14), $N_3 = 36$. Thus, based on (14), the worst-case length of the base ring is lower bounded by 36 hops. However, as k exceeds a certain threshold, a worst-case path due to (9) will be longer than that due to (13). Specifically, when $k = 3$, $N_{max}^k = \max\{N_2, N_3\} = \max\{64, 60\} = 64$; when $k = 4$, $N_{max}^k = \max\{N_2, N_3\} = \max\{84, 78\} = 84$. As k increases further, the gap between N_2 and N_3 will keep increasing.

References

1. Yu, S., Zhang, B., Yao, Z., Li, C.: R3: a lightweight reactive ring based routing protocol for wireless sensor networks with mobile sinks. KSII Trans. Internet Inf. Syst. **10**(12), 5442–5463 (2016)
2. Wang, G., Wang, T., et al.: Adaptive location updates for mobile sinks in wireless sensor networks. J. Supercomput. **47**(2), 127–145 (2009)
3. Yu, F., Park, S., et al.: Elastic routing: a novel geographic routing for mobile sinks in wireless sensor networks. IET Commun. **4**(6), 716–727 (2010)
4. Zhao, Z., Zhang, B., et al.: Providing scalable location service in wireless sensor networks with mobile sinks. IET Commun. **3**(10), 1628–1637 (2009)
5. Yan, Y., Zhang, B., et al.: Hierarchical location service for wireless sensor networks with mobile sinks. Wirel. Commun. Mob. Comput. **10**(7), 899–911 (2010)
6. Tian, K. Zhang, B., et al.: Data gathering protocols for wireless sensor networks with mobile sinks. In: Proceedings of IEEE GLOBECOM 2010, pp. 1–6. IEEE Press, Miami, FL (2010)
7. Shi, L., Yao, Z., Zhang, B., Li, C., et al.: An efficient distributed routing protocol for wireless sensor networks with mobile sinks. Int. J. Commun. Syst. **28**(11), 1789–1804 (2015)
8. Shi, L., Zhang, B., et al.: An efficient multi-stage data routing protocol for wireless sensor networks with mobile sinks. In: Proceedings of IEEE Globecom 2011, pp. 1–5, Houston, TX (2011)
9. Shi, L., Zhang, B., et al.: DDRP: an efficient data-driven routing protocol for wireless sensor networks with mobile sinks. Int. J. Commun. Syst. **26**(10), 1341–1355 (2013)